



Murdoch
UNIVERSITY

MURDOCH RESEARCH REPOSITORY

This is the author's final version of the work, as accepted for publication following peer review but without the publisher's layout or pagination.

The definitive version is available at

<http://dx.doi.org/10.1016/j.firesaf.2012.03.004>

El-Harbawi, M., Shaaran, S.N.A.Bt.S., Ahmad, F., Wahi, M.A.A., Abdul, A., Laird, D.W. and Yin, C-Y (2012) *Estimating the flammability of vapours above refinery wastewater laden with hydrocarbon mixtures.* Fire Safety Journal, 51 . pp. 61-67.

<http://researchrepository.murdoch.edu.au/8075/>

Copyright: © 2012 Elsevier Ltd.

It is posted here for your personal use. No further distribution is permitted.

1 **Estimating the flammability of vapours above refinery waste**
2 **water laden with hydrocarbons mixtures**

3
4 Mohanad El-Harbawi^{1,*}, Siti Nurul Asikhin Bt. Shaaran², Fatihah Ahmad¹, Muhammad
5 Aizat Abd Wahid¹, Adamu Abdul³, Damian W. Laird⁴, Chun-Yang Yin⁴

6
7 *¹Department of Chemical Engineering, Universiti Teknologi PETRONAS, 31750, Tronoh, Perak,*
8 *Malaysia*

9 *²Reliability Integrity Engineering, Petronas Carigali Sdn Bhd, Petronas, Jln Belia, 88000 Kota Kinabalu,*
10 *Sabah, Malaysia*

11 *³Department of Chemical Engineering, Universiti Teknologi Malaysia, 81310, Skudai, Johor-Bahru,*
12 *Malaysia*

13 *⁴School of Chemical and Mathematical Sciences, Murdoch University, Murdoch, 6150, Western Australia*

14
15
16 *Corresponding author: Tel: +605-3687581, Email: mohanad_elharbawi@petronas.com.my*

24 **Abstract**

25

26 In this study, the likelihood of fire hazards attributed to the vaporization of hydrocarbon
27 components derived from refinery wastewater drainage systems was assessed. Liquid samples
28 containing mixtures of hydrocarbon products and water were collected from a refinery drainage
29 system and subjected to a distillation process to separate oil and water. The oil-liquid phase was
30 analyzed using Gas Chromatography Mass Spectrometry (GC-MS) to examine the composition
31 of the sample. Hydrocarbon compounds ranging from C₉ to C₁₆ were detected. Mole fractions of
32 28 selected components in the liquid phase were obtained from the GC-FID data and used to
33 calculate mole fractions of components in the gas phase via modified Raoult's law. Lower
34 Flammability Limits (*LFLs*) and Upper Flammability Limits (*UFLs*) for individual components
35 were calculated using a stoichiometric concentration method, while the *LFL* and *UFL* values for
36 the mixture (*LFL_{mix}* and *UFL_{mix}*) were calculated using the Le Chatelier equation. The *LFL_{mix}*
37 and *UFL_{mix}* values were used to construct a flammability diagram and subsequently used to
38 determine the flammability of the mixture. The findings of this study may assist in minimizing
39 fire hazards associated with presence of hydrocarbon vapours derived from refinery wastewater
40 streams.

41

42 **Keywords:** Gas chromatography; compositions; Lower and Upper Flammability Limits;
43 flammability diagram.

44

45

46

47 **1. Introduction**

48

49 Refineries are complex systems of numerous chemical process operations that refine crude
50 oil into desired products such as Liquefied Petroleum Gas (LPG), petrochemical naphtha, motor
51 gasoline, kerosene, diesel and other products. Petroleum refineries can consume high quantities
52 of water for operational usage relative to other industrial and domestic users within a
53 geographical region. Consequently, these refineries can generate large volumes of wastewaters
54 containing various petroleum hydrocarbons, heavy metals, sulfur and ammonia at concentrations
55 that typically require treatment (Al-Haddad et al., 2007) prior to final discharge. With respect to
56 hydrocarbon components, highly flammable compounds such as benzene, toluene, ethylbenzene
57 and xylenes may be present and they pose a significant threat of fire hazard. Over time, the
58 mixture of water and hydrocarbon in drainage systems at certain conditions will naturally
59 separate and form distinct liquid phases, based on density and polarity of the material (EPA,
60 1998). Hydrocarbon compounds from these drainage flows can vary widely in composition from
61 day-to-day due to operational activities such as storage of waste liquids from drains, equipment
62 cleaning and spills. Some of these compounds can evaporate and turn into vapour at ambient
63 temperature and atmospheric pressure, thus creating potentially flammable mixtures in air. The
64 presence of flammable mixtures exposes drainage systems to the possibility of fire and
65 explosion.

66 The composition of hydrocarbon compounds can be determined and ignitable liquids can be
67 identified (Newman et al, 1997) using comprehensive gas chromatography (GC) systems such as
68 gas chromatography–isotope ratio mass spectrometry (GC–IRMS) and gas chromatography–mass
69 spectrometry (GC-MS). GC analysis can determine the presence, type and concentrations of

70 contaminated hydrocarbons in wastewater (Senn and Johnson, 1987). However, GC analysis of
71 sample compositions is not sufficient to predict the flammability of hydrocarbon mixtures. In this
72 regard, a flammability diagram method can be suitably used for this purpose (Mashuga and
73 Crowl, 1999). Flammability diagrams generally show the “area” of flammability in mixtures of
74 fuel, oxygen and an inert gas. Mixtures of the three gases are usually depicted in a triangular
75 diagram, also known as a Ternary plot. For more detailed information on the ignitability of
76 mixtures and spark ignition, readers are directed to reviews by Mullins (1955), Lewis and von
77 Elbe (1987), and Mullins and Penner (1959).

78 Vapour-air mixtures ignite and burn only over a well-specified range of compositions. The
79 mixture will not burn when the composition is lower than the lower flammable limit (LFL), that
80 is, the mixture is too lean for combustion. The mixture is also not combustible when its
81 composition is too rich, that is, when it is above the upper flammable limit (UFL). As such, a
82 mixture is flammable only when its composition is between LFL and UFL. These flammability
83 limits can be measured experimentally, though they can still be determined without experimental
84 data (Crowl and Louvar, 2002). There are several available methods, databases and software
85 packages that provide sufficient flammability information for various hydrocarbons and they can
86 be sourced from Coward and Jones (1952), Zabetakis (1965), Sax (1984), Kuchta (1985), Ohtani
87 *et al.* (1994), Brooks and Crowl (2007a) and DIPPR (2010).

88 The limiting oxygen concentration (LOC) is defined as the minimum oxygen concentration
89 in a mixture of fuel, air and inert gas that will propagate flame and is expressed in volume
90 percent of oxygen (Zlochower and Green, 2009). In essence, LOC varies with pressure and
91 temperature and depends on the type of inert (non-flammable) gas present. A reaction can not
92 generate enough energy to heat the entire gas mixture required for the self-propagation of the

93 flame if the oxygen concentration is below the LOC (Crowl and Louvar, 2002). As such, the
94 LOC is a useful parameter in terms of fire hazard prevention since explosions and fires can be
95 prevented by reducing the oxygen concentration regardless of fuel concentration. This concept is
96 the basis for a common procedure called *inerting* used in safety engineering (Crowl and Louvar
97 2002; ASTM 2009). The LOC can be measured experimentally using a flammability apparatus
98 (British and European Standard, 2007; ASTM 2008a; ASTM 2008b) or it can be found from
99 different resources (NFPA 1994; CHEMSAFE, 2007). An example of experimental LFL and
100 LOC determination can be found from a study conducted by Brooks and Crowl (2007b), in
101 which they experimentally measured the LFL, LOC and the maximum safe solvent concentration
102 (MSSC) for ethanol and acetonitrile above aqueous solutions. If experimental and/or literature
103 data are not available, the LOC can be estimated using the stoichiometric combustion reaction
104 and the LFL. This procedure works relatively well for many different hydrocarbons (Siwek,
105 1996; Crowl and Louvar, 2002).

106 The objectives of this study were to estimate flammability limits and the LOC of the
107 hydrocarbon vapour mixture above refinery wastewater and subsequently determine the
108 flammability of the mixture. This was achieved by incorporating thermodynamics with process
109 safety concepts. Findings from this study can be used to investigate the root cause of fire
110 incidents in drainage systems due to the presence of flammable hydrocarbon vapour mixtures.

111

112

113

114

115

116 2. Methodology

117

118 2.1.1 *Liquid Phase*

119

120 Liquid samples were collected from drainage lines in a refinery located in Malaysia.

121 Residual water was removed from the samples using a simple distillation technique. The

122 composition of the organic-phase liquid was analysed using both GC-MS (for identification) and

123 GC-FID (Flame Ionisation Detection) (for quantitation). GC-MS was performed with a

124 Shimadzu QP5050 GCMS using the following settings: Electron impact ionization, electron

125 energy 70 eV and scan range 40 - 500 amu at 1 scan/s. The carrier gas (Helium 99.999%) flow

126 rate was set to 1.5 ml/min with column inlet pressure 54.8 kPa and linear velocity 36.10 cm/sec.

127 The end of the column was directly introduced into the ion source of a mass selective detector

128 operated in an electron impact ionization mode. Samples were injected into a HP5 fused silica

129 (5% phenyl polysilphenylene-siloxane) capillary column BPX5 (30 m length; 0.25 mm i.d.; 0.25

130 μm film thickness) and the oven temperature was held at 55^o C for 2 min. It was then increased to

131 300^oC at 5^oC/min and thereafter held for 40 minutes. The components of the liquid sample were

132 identified by comparing their mass spectra with the NIST Mass Spectral Database. Pure samples

133 of a selected number of compounds were analysed using the same GCMS conditions in order to

134 verify the match from the database.

135 Quantitative analysis of the peaks was performed with a Shimadzu GC2010 with an FID using

136 the same column and temperature parameters as for the GC-MS analysis.

137 The mass fraction of each component in the liquid phase can be determined from GC-FID data

138 (Eq. 1):

139
$$\chi_i = \frac{A_i}{A_T} \quad (1)$$

140 where, χ_i is the mass fraction of component i , A_i is the peak area of component i , and A_T is the
141 peak area of all components.

142

143 The mass fraction is converted to mole fraction using Eq. (2):

144
$$x_i = \frac{\chi_i/M_i}{\sum \chi_i/M_i} \quad (2)$$

145 where, x_i is the mole fraction in liquid phase of component i , and M_i is the molecular weight of
146 component i .

147

148 2.1.2 Vapour Phase

149

150 It was necessary to estimate the concentrations of components in the gas phase, which also
151 contributed to the flammability of the mixture. Modified Raoult's law was used to estimate the
152 amount of liquid vaporized at ambient temperature; Eq. (3) was used to calculate the mole
153 fraction in the gas phase.

154
$$\gamma_i x_i P_i^{sat} = \phi_i y_i P_t \quad (3)$$

155 where γ_i is the activity coefficient for component i , x_i is the mole fraction of in the liquid
156 phase, P_i^{sat} is the vapour pressure of compound i as a pure component, ϕ_i is the fugacity
157 coefficient for component i , y_i is the mole fraction of component i in the vapour phase, and P_t is
158 the total pressure. Theoretically, the activity coefficient, γ_i , for an ideal solution is equal to 1.

159 However, since the mixture is non-ideal (real), the activity coefficient was calculated using the

160 UNIversal Functional Activity Coefficient (UNIFAC) method. The UNIFAC method expresses
 161 the activity coefficient as the sum of a combinatorial part, $\ln \gamma_i^C$ and a residual part, $\ln \gamma_i^R$ (Eq.
 162 4) (Fredenslund et al., 1975):

$$163 \quad \ln \gamma_i = \ln \gamma_i^C + \ln \gamma_i^R \quad (4)$$

164 $\ln \gamma_i^C$ is given by Eq. (5):

$$165 \quad \ln \gamma_i^C = \ln \frac{\Phi_i}{x_i} + \frac{z}{2} q_i \cdot \ln \frac{\theta_i}{\Phi_i} + l_i + \frac{\Phi_i}{x_i} \sum_{j=1}^M x_j \cdot l_j \quad (5)$$

$$166 \quad l_j \equiv \frac{z}{2} (r_j - q_j) - (r_j - 1) \quad (6)$$

167 Where z is the average number of nearest neighbours around a group in solution (constant value
 168 is used: $z = 10$). The segment fraction, Φ_i , and surface area fraction, θ_i , are defined, respectively
 169 by Eqs. (7) and (8):

$$170 \quad \Phi_i = \frac{r_i x_i}{\sum_{j=1}^M r_j x_j} \quad (7)$$

$$171 \quad \theta_i = \frac{q_i x_i}{\sum_{k=1}^M q_k x_k} \quad (8)$$

172 The molecular volume, r_j , is defined by the sum of its constituent group given by Eq. (9):

$$173 \quad r_j = \sum_{k=1}^N v_k^j \cdot R_k \quad (9)$$

174 Where v_k^j is the number of k groups in molecule j , and R_k is the volume of group k . The
 175 molecular surface area, q_j , is the sum of the individual group areas in the molecules given by Eq.
 176 (10):

177
$$q_j = \sum_{k=1}^N v_k^j \cdot Q_k \quad (10)$$

178 where Q_k is the group surface area.

179 R_k and Q_k are obtained from the van der Waals group volumes and surface areas.

180 $\ln \gamma_i^R$ was calculated from Eq. (11):

181
$$\ln \gamma_i^R = \sum_{k=1}^N v_k^i [\ln \Gamma_k - \ln \Gamma_k^i] \quad (11)$$

182 where Γ_k^i is the group residual activity coefficient of group k in a reference solution containing

183 only molecules of type i . Γ_k is the group residual activity coefficient in the solution. The

184 coefficients Γ_k^i and Γ_k are related to the composition and temperature according to Eq. (12):

185
$$\ln \Gamma_k = Q_k \left\{ 1 - \ln \left(\sum_{m=1}^N \Theta_m \cdot \psi_{mk} \right) - \sum_{m=1}^N \left[\frac{\Theta_m \cdot \psi_{km}}{\sum_{n=1}^N \Theta_n \cdot \psi_{nm}} \right] \right\} \quad (12)$$

186 In Eq. (12), the group interaction parameter, ψ_{mk} is defined by Eq. (13):

187
$$\psi_{mk} = e^{-\frac{a_{mk}}{T}}, \quad a_{mk} \neq a_{km} \quad (13)$$

188 where a_{mk} is the group interaction parameter between groups n and m . The surface contribution,

189 Θ_m and the mole fraction of the group, X_m are defined by Eqs. (14) and (15), respectively:

190
$$\Theta_m \equiv \frac{Q_m \cdot X_m}{\sum_{n=1}^N Q_n \cdot X_n} \quad (14)$$

191
$$X_m \equiv \frac{\sum_{j=1}^M v_m^j \cdot x_j}{\sum_{j=1}^M \sum_{n=1}^N v_n^j \cdot x_j} \quad (15)$$

192 The fugacity coefficient, φ_i , for each component in the mixture was determined using the Peng-
 193 Robinson method (Eq. (16) (Peng and Robinson, 1976):

$$194 \quad \ln\varphi_i = \frac{b_k}{b}(Z-1) - \ln(Z-B) - \frac{A}{2\sqrt{2B}} \times \left(\frac{2\sum_i^N x_i a_{ik}}{a} - \frac{b_k}{b} \right) \ln\left(\frac{Z+2.414B}{Z-2.414B} \right) \quad (16)$$

195 where φ_i is the fugacity coefficient, b is van der Waals co-volume defined by Eq. (17), Z is the
 196 compressibility factor defined by Eq. (18), B is a constant defined by Eq. (19), A is a constant
 197 defined by Eq. (20), x_i is the mole fraction, and a is the attraction parameter defined by Eq.
 198 (21):

$$199 \quad b = \sum_i^N x_i b_i \quad (17)$$

$$200 \quad Z = \frac{Pv}{RT} \quad (18)$$

$$201 \quad B = \frac{bP}{RT} \quad (19)$$

$$202 \quad A = \frac{aP}{R^2T^2} \quad (20)$$

$$203 \quad a = \sum_i^N \sum_j^N x_i x_j a_{ij} \quad (21)$$

204 where P is the pressure defined by Eq. (22), T is the temperature, v is the molar volume, R is the
 205 universal gas constant, a_{ij} is defined by Eq. (23), and i, j, k are component identifications.

$$206 \quad P = \frac{RT}{v-b} - \frac{a(T)}{v^2 + 2bv - b^2} \quad (22)$$

$$207 \quad a_{ij} = (1 - \delta_{ij}) a_i^{1/2} a_j^{1/2} \quad (23)$$

208 where, δ_{ij} is an empirically determined binary interaction coefficient for components i and j .

209 Applying Eq. (24) at the critical point, we obtain:

$$210 \quad a(T_c) = 0.45724 \frac{(RT_c)^2}{P_c} \quad (24)$$

$$211 \quad b(T_c) = 0.07780 \frac{RT_c}{P_c} \quad (25)$$

$$212 \quad Z_c = 0.307$$

213 At temperatures other than the critical:

$$214 \quad a(T) = a(T_c) \cdot a(T_r, \omega) \quad (26)$$

$$215 \quad b(T) = b(T_c) \quad (27)$$

216 where $a(T_r, \omega)$ is a dimensionless function of reduced temperature and acentric factor, ω and

217 equals unity at the critical temperature.

218 The total pressure for the mixture can be calculated from Eq. (28):

$$219 \quad P_t = \sum \gamma_i x_i P_i^{sat} \quad (28)$$

220 The vapour pressures of the components were calculated using the classic (Eq. 29) and extended

221 Antoine equations (Eq. 30):

$$222 \quad \log_{10} P^{sat} = A - \frac{B}{C + T} \quad (29)$$

$$223 \quad \log_{10} P^{sat} = A - \frac{B}{T} + C \log_{10} T + DT + ET^2 \quad (30)$$

224 where

225 P^{sat} is the vapour pressure (mmHg) while A , B , C , and D are the component-specific constants.

226 These constants were obtained from several sources (Wichterle and Linek, 1971; Yaws, 1992;

227 Dykyj et al., 1999; Yaws et al., 2009; www.chemspider.com).

228 2.2.1 *LFL and UFL*

229 For some situations, it may be necessary to estimate the flammability limits without
 230 experimental studies. Jones (1938) found that for many hydrocarbon vapours, the *LFL* and *UFL*
 231 were functions of the stoichiometric concentration of fuel (C_{st}) (Eq. 31 and Eq. 32):

232
$$LFL = 0.55C_{st} \quad (31)$$

233
$$LFL = 3.5C_{st} \quad (33)$$

234 The stoichiometric concentration, C_{st} for organic compounds was determined using the general
 235 combustion reaction (Eq. 33).



237 where z is equivalent moles O_2 /moles fuel which can be determined from Eq. (34):

238
$$z = m + \frac{x}{4} - \frac{y}{2} \quad (34)$$

239 The stoichiometric concentration, C_{st} can be determined as a function of z by Eq. (35):

240
$$C_{st} = [\text{moles fuel} / (\text{moles fuel} + \text{moles air})] \times 100 = \frac{100}{[1 + (z/0.21)]} \quad (35)$$

241 Substituting Eq. (34) into Eq. (35) and applying Eq. (31) and Eq. (32) yield Eqs. (36) and (37):

242
$$LFL(\text{vol } \%) = \frac{0.55(100)}{4.76m + 1.19x - 2.38y + 1} \quad (36)$$

243
$$UFL(\text{vol } \%) = \frac{3.50(100)}{4.76m + 1.19x - 2.38y + 1} \quad (37)$$

244 where *LFL* and *UFL* are the lower and upper flammable limits, respectively.

245 The *LFL* and *UFL* for mixtures (LFL_{mix} and UFL_{mix}) were calculated using the Le Chatelier

246 equation (Eqs. 38 and 39) (Le Chatelier, 1891):

247
$$LFL_{mix} (vol\%) = \frac{1}{\sum(y_i/LFL_i)} \quad (38)$$

248
$$UFL_{mix} (vol\%) = \frac{1}{\sum(y_i/UFL_i)} \quad (39)$$

249 where LFL_i and UFL_i are the lower and upper flammable limits, respectively, for component i in
 250 fuel and air while n represents the number of combustible species.

251

252 2.2.2 Limiting Oxygen Concentration (LOC)

253

254 LOC can be estimated using the stoichiometry of the combustion reaction and the LFL
 255 (Crowl and Louvar, 2002). Eq. (40) can also be used to estimate LOC for a vapour mixture
 256 (Zlochower and Green, 2009):

257
$$LOC_{mix} = \sum y_i R_i / \sum y_i / L_i^* = \sum y_i R_i / \sum y_i R_i / LOC_i \quad (40)$$

258
$$L_i^* = LOC_i / R_i \quad (41)$$

259 where LOC_{mix} is the limiting oxygen concentration for the vapour mixture (vol%), R_i is the
 260 stoichiometric molar ratio of oxygen to compound i in the vapour phase, and LOC_i is the
 261 limiting oxygen concentration for individual compound (vol%). Figure 1 shows the methodology
 262 outline adopted in this study.

263

264

265

266

267

268 3. Results and Discussion

269

270 3.1 Compositions

271

272 The components were identified using a combination of the retention time, comparison of
273 mass spectrum derived from GC-MS analysis of the hydrocarbon mixture to a mass spectral
274 library, and comparison to known standards. Figure 2 shows the retention time and peak
275 abundance data for 77 components detected in the liquid phase via GC-MS analysis. Considering
276 the difficulties of relying solely on mass spectral database matching for the identification of
277 compounds that are very similar in molecular structure, it was felt prudent to take the following
278 precautions in deciding which of the 77 individual compounds observed in the gas
279 chromatogram should be used in calculations. Firstly, using pure compounds that were readily
280 available it was ascertained that peaks 3, 14, 41, 52, 75, and 77 were simple straight chain
281 hydrocarbons (Table S1 - electronic Supplementary material) and that the compound ID from the
282 NIST database matched with the compounds injected. These results confirmed that the output
283 from the mass spectral comparison was valid, particularly for compounds with higher than 95%
284 match. Subsequently, all compounds with a minimum 95% database match were considered to
285 have been correctly identified. As a check on this assumption it was noted that the database
286 identification of peaks 28, 42, 50, and 63 were for simple straight chain alkanes and produced a
287 homologous series with the positively identified compounds. Additionally, it was noted that the
288 difference in retention times between these compounds, running from nonane to hexadecane,
289 were consistent providing further evidence that these were compounds of a homologous
290 hydrocarbon series. There are 28 compounds (Table S1- also contains the properties relevant for

291 this study) that meet the above criteria and their order of elution based on their boiling points,
292 (i.e. those with higher boiling points elute later) is also consistent with expected results. These
293 selected 28 compounds cover all the major identified peaks (including numbers 42, 50, 63) and
294 account for a 56% of the total area in the chromatogram (as determined from GC-FID data).

295 The identification of individual components shows that the liquid sample contains a large
296 number of hydrocarbon components ranging from C₉ to C₁₆. The predominant hydrocarbon
297 groups are alkane and alkene with a relatively minor presence of arenes. The peak numbers 14,
298 28, 41, 52, 65, and 75 are assigned to decane, undecane, dodecane, tridecane, tetradecane, and
299 pentadecane, respectively, and these six components constitute more than 43% of the total
300 chromatogram area,. The mass fraction of each component was estimated by dividing the GC-
301 FID peak area of each component by the total peak area. The mass fraction was then converted to
302 mole fraction according to Eq. (2) and the resulting distribution for the mole fraction for each
303 component x_i in the liquid phase is shown in Figure 3.

304

305 3.2 *Mole Fraction in Vapour Phase*

306

307 The activity and fugacity coefficients for all components in the vapour mixture are
308 calculated and the values shown in Table S1. The average activity and fugacity coefficients for
309 the vapour mixture were determined to be 1.02 and 0.88 respectively. Figure 4 shows the mole
310 fraction for each component in the vapour phase, y_i based on combustible basis. Interestingly, the
311 values of y_i for most components are small; possibly due to the low volatility of the heavy
312 hydrocarbon components detected in the liquid phase. The low volatilities of the components
313 were due to the low vapour pressure, which range from 5×10^{-3} mmHg to 6.74 mmHg. The total

314 mole fraction of the vapour mixture is 0.12 vol %, while the air content in the mixture is 99.88
315 vol%. Therefore, the percentages of N₂ and O₂ in the mixture are approximated to be 79 vol%
316 and 21 vol%, respectively.

317

318 3.3 *LFL, UFL, and LOC*

319

320 The calculated *LFL* and *UFL* as well as *LOC* values are listed in Table S1. The calculated
321 *LFL* and *UFL* values are in agreement with those obtained from other databases and open
322 literatures (Figures 5a and 5b). It should be noted that not all *LFL* and *UFL* values could be
323 found in other database and published literatures and some of these values were not indicated in
324 Table S1. The *LFL_{mix}* and *UFL_{mix}* are determined to be 0.72 vol% and 4.60 vol%, respectively
325 while the *LOC_{mix}* value is 11.40 vol%.

326

327 3.4 *Flammability Diagram*

328

329 A flammability diagram is a conventional method used to assess the flammability of mixture
330 of gases. The flammability diagram is represented by three axes, namely, (1) fuel (hydrocarbon
331 vapour mixture), (2) inert material, and (3) oxygen. In order to plot the flammability diagram,
332 concentrations of the fuel, oxygen, and inert material (in volume or mole %) are required. The air
333 line is plotted by taking the compositions of air from Table S1 (78.91 % nitrogen and 20.98 %
334 oxygen). The intersection of the stoichiometric line with the oxygen axis is given by $100(z/1+z)$
335 (Crowl and Louvar, 2002). The *LOC_{mix}* line can be drawn by locating the *LOC_{mix}* value (11.40%)
336 on the air axis and then drawing a parallel line until it intersects with the stoichiometric line. To

337 construct the flammability zone, the values of LFL_{mix} and UFL_{mix} are required and they are
338 located on the air line while the flammability zone is the area to the right of the air line. Figure 6
339 represents the triangular flammability diagram for the hydrocarbon mixture. It can be clearly
340 seen that the stoichiometric line crosses the flammable zone. Therefore, it can be inferred that the
341 vapour mixture is flammable.

342

343 **4. Conclusions**

344

345 In this study, theoretical work including thermodynamic fundamentals and flammability
346 calculations were applied to estimate the flammability limits of hydrocarbon vapours derived
347 from refinery wastewater. Detailed inspection of the customised flammability diagram showed
348 that the vapour mixture derived from the wastewater was flammable and may pose a potential
349 fire hazard. As such, it is always prudent for refinery workers to exercise caution when handling
350 wastewater laden with hydrocarbon residuals. Findings from this study afford a useful basis for
351 safety officers and engineers from other refineries to assess the potential fire hazards associated
352 with hydrocarbon vapours derived from wastewater streams.

353

354 **References**

355

356 Al-Haddad A., Chmielewska E., and Al-Radwan S., (2007). A Brief Comparable Lab
357 Examination for Oil Refinery Wastewater Treatment using the Zeolitic and Carbonaceous
358 Adsorbents. *Petroleum & Coal* 49 (1): 21-26.

359

360 ASTM (2008a). Standard test method for concentration limits of flammability
361 of chemicals (vapors and gases). E681-04. In: ASTM International annual book of standards,
362 Vol. 14.02. West Conshohocken, PA: American Society for Testing and Materials.
363

364 ASTM (2008b). Standard test methods for limiting oxygen (oxidant) concentration in gases and
365 vapors. E2079-07. In: ASTM International annual book of standards, Vol. 14.02. West
366 Conshohocken, PA: American Society for Testing and Materials.
367

368 ASTM (2009). Standard Test Method for Measuring the Minimum Oxygen Concentration to
369 Support Candle-Like Combustion of Plastics (Oxygen Index). D2863-09. *American Society for*
370 *Testing and Materials (ASTM)*.
371

372 British and European Standard. (2007). Determination of limiting oxygen concentrations of
373 gases and vapours. EN 14756. rue de Stassart, 36, B-1050 Brussels, Belgium: CEN European
374 Committee for Standardization.
375

376 Brooks, M., Crowl, D., (2007a). Flammability Envelopes for Methanol, Ethanol, Acetonitrile and
377 Toluene. *Journal of Loss Prevention in the Process Industries* 20: 144–150.
378

379 Brooks, M., Crowl, D., (2007b). Vapor Flammability above Aqueous Solutions of Flammable
380 Liquids. *Journal of Loss Prevention in the Process Industries* 20: 477–485.
381

382 CHEMSAFE, (2007). Database of evaluated safety characteristics. Frankfort/M, Germany:
383 DECHEMA, BAM, and PTB.
384
385 ChemSpider (Database of Chemical Structures and Property Predict.
386 www.chemspider.com
387
388 Coward, H. F. and Jones, G. W., (1952). Limits of Flammability of Gases and Vapors. *Bulletin*
389 *503, Bureau of Mines.*
390
391 Crowl D., A, Louvar J. F., (2002). Chemical Process Safety: fundamentals with applications.
392 *Prentice-Hall.*
393
394 DIPPR, (2010). DIPPR® Project 801. Evaluated Standard Thermophysical Property Values.
395 American Institute of Chemical Engineers Design Institute for Physical Properties.
396
397 Dykyj J., Svoboda J., Wilhoit R., Frenkel M., Hall K., (1999). Vapor Pressure of Chemicals.
398 *Springer, Vol. 20.*
399
400 EPA, (1998). EPA Chemical Accident Investigation Report. *United States Environmental*
401 *Protection Agency.*
402
403 Fredenslund, A. Jones, R. L. Prausnitz, J. M., (1975). Group-Contribution Estimation of Activity
404 Coefficients in Nonideal Liquid Mixtures. *AIChE J.* 21: 1086–1099.

405 Jones, G. W., (1938). Inflammation Limits and their Practical Application in Hazardous
406 Industrial Operations. *Chemical Reviews*, 22 (1): 1-26.
407
408 Kuchta, J. M., (1985). Investigation of Fire and Explosion Accidents in the Chemical, Mining,
409 and Fuel-related Industries-A manual. *Bureau of Mines Bulletin*, 680.
410
411 Le Chatelier H., (1891). Estimation of Firedamp by Flammability Limits. *Ann. Mines*, ser. 8, 19:
412 388-395.
413
414 Lewis, B., von Elbe, G., (1987). Combustion Flames and Explosions of Gases. *Academic Press*,
415 pp 731.
416
417 Mashuga, C. and Crowl D., (1999). Flammability Zone Prediction Using Calculated Adiabatic
418 Flame Temperatures. *Process Safety Progress*, 18 (3): 127-134,
419
420 Mullins, B. P, (1955). Spontaneous Ignition of Liquid Fuels. *Butterworths Scientific*
421 *Publications*, London, pp. 117.
422 Mullins B. P., and Penner, S. S., (1959). Explosions, Detonation, Flammability and Ignition.
423 *Pergamon Press, Inc.*, New York, pp. 199.
424
425 Newman R., Gilbert, M., Lothridge, K., (1997). GC-MS Guide to Ignitable Liquids. CRC-Press.
426
427 NFPA 68, Venting of Deflagrations (Quincy, MA: National Fire Protection Association, 1994).

428 Ohtani, H., Lee, S. G., and Uehara, Y., (1994). Combustion Characteristics of Several
429 Flammable Gases with Chlorine Trifluoride. *Proceedings of the Fourth International Symposium*
430 *on Fire Safety Science, Ottawa, Canada.*
431

432 Peng, D. Y., and Robinson, D. B. (1976). A New Two-Constant Equation of State. *Ind. Eng.*
433 *Chem. Fundam.*, 15 (1): 59-64.
434

435 Sax, N. I., (1984). Dangerous Properties of Industrial Materials. *New York: Van Nostrand*
436 *Reinhold Co.*
437

438 Senn, R., and Johnson, M., (1987). Interpretation of Gas Chromatographic Data in Subsurface
439 Hydrocarbon Investigations. *Ground Water Monitoring & Remediation*, 7(1): 58–63.
440

441 Siwek, R., (1996). Determination of Technical Safety Indices and Factors Influencing Hazard
442 Evaluation of Dusts. *Journal of Loss Prevention in the Process Industries*, 9(1): 21-31.
443

444 Wichterle, I., Linek, J., (1971). Antoine vapor pressure constants of pure compounds. *Academia,*
445 *Prague.*
446

447 Yaws, C. L., Narasimhan, P. K., Gabbula Chaitanya, (2009). Yaws' Handbook of Antoine
448 Coefficients for Vapor Pressure. *Knovel library.*
449

450 Yaws, C. L., (1992). Handbook of Thermodynamic Diagrams, Organic Compound C₈ to C₂₈,
451 Vol. 3 (Library of Physico-Chemical Property Data). *Gulf Professional Publishing*.

452

453 Zabetakis, M. G. (1965). Flammability Characteristics of Combustible Gases and Vapors.
454 *Bulletin 627, Bureau of Mines*.

455

456 Zlochower, I., Green, G., (2009). The Limiting Oxygen Concentration and Flammability Limits
457 of Gases and Gas mixtures. *Journal of Loss Prevention in the Process Industries* 22: 499-505.

458

459

460

461

462

463

464

465

466

467

468

469

470

471

472

473 **Figure Captions**

474

475 **Fig.1.** Flowchart on the methodology used in this study.

476 **Fig. 2.** GC analysis for the liquid sample.

477 **Fig. 3.** Percentages of hydrocarbon mole fractions in the liquid phase.

478 **Fig. 4.** Percentages of hydrocarbon mole fractions in the vapour phase.

479 **Fig. 5a&b.** Comparison between calculated and literature values of *LFL* and *UFL*.

480 **Fig. 6.** Triangular flammability diagram of the hydrocarbon mixture.

481

482

483

484

485

486

487

488

489

490

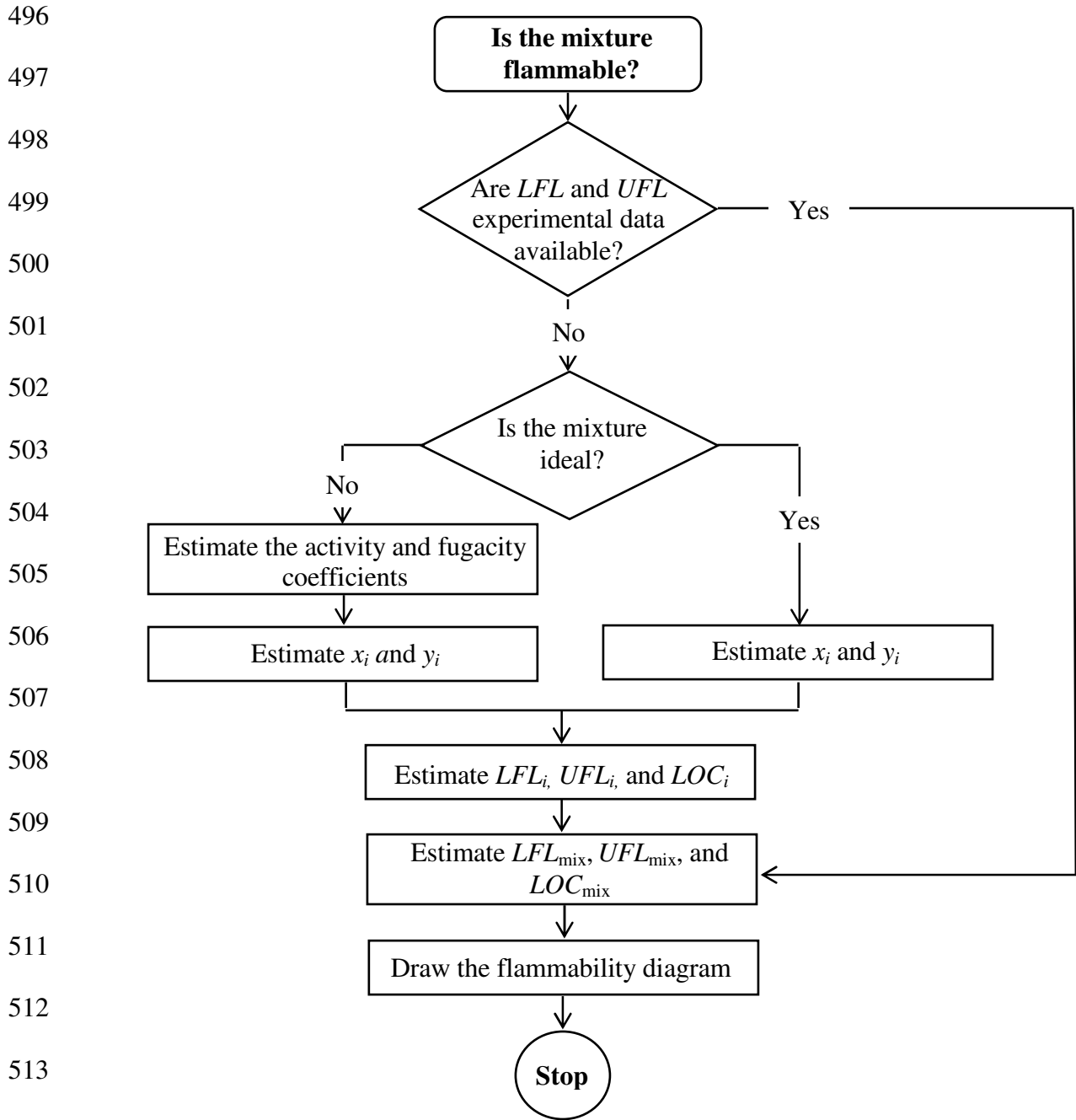
491

492

493

494

495

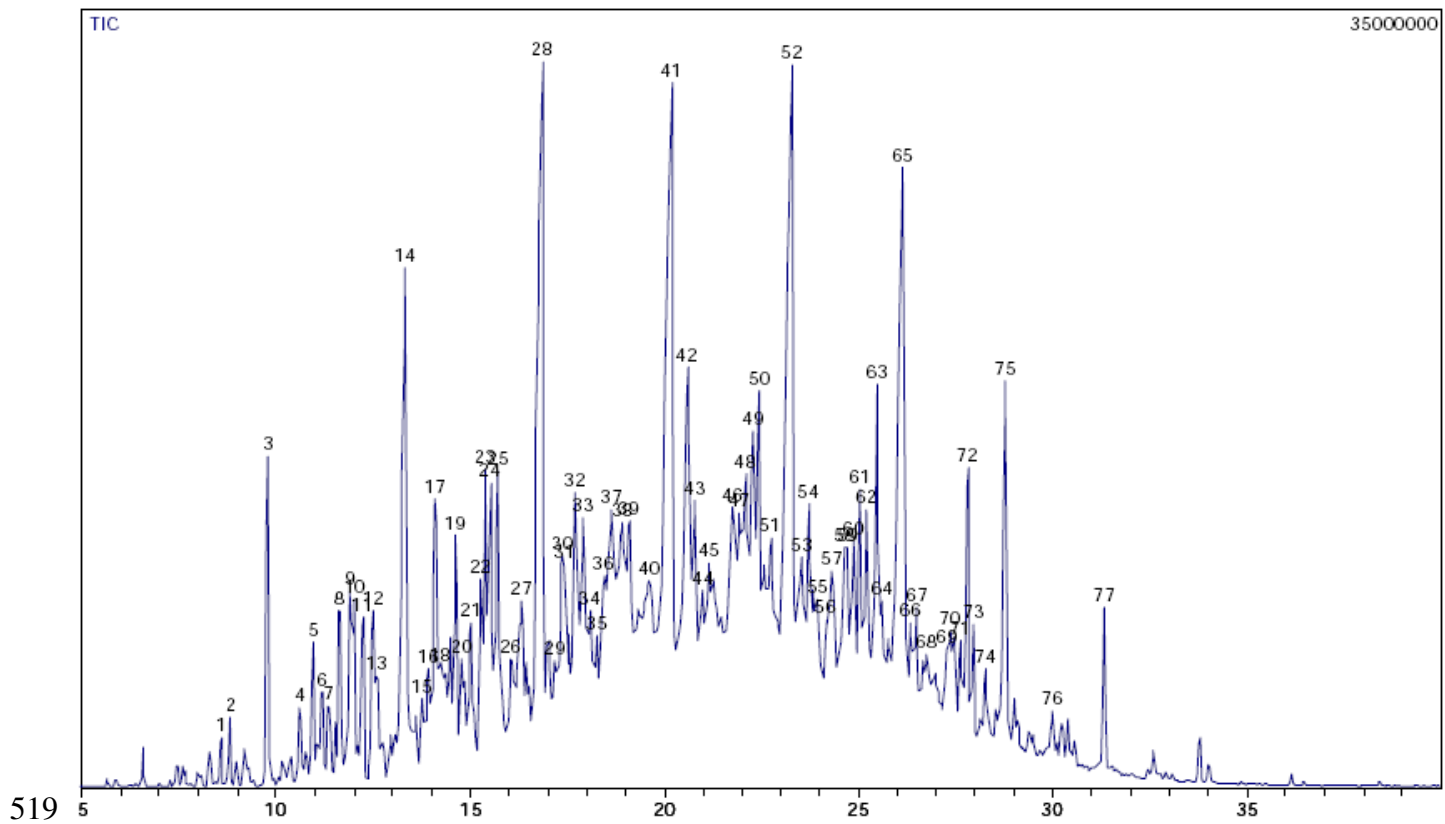


515 **Fig. 1:** Flowchart on the methodology used in this study.

516

517

518



519

520

Fig. 2. GC-MS analysis for the liquid sample.

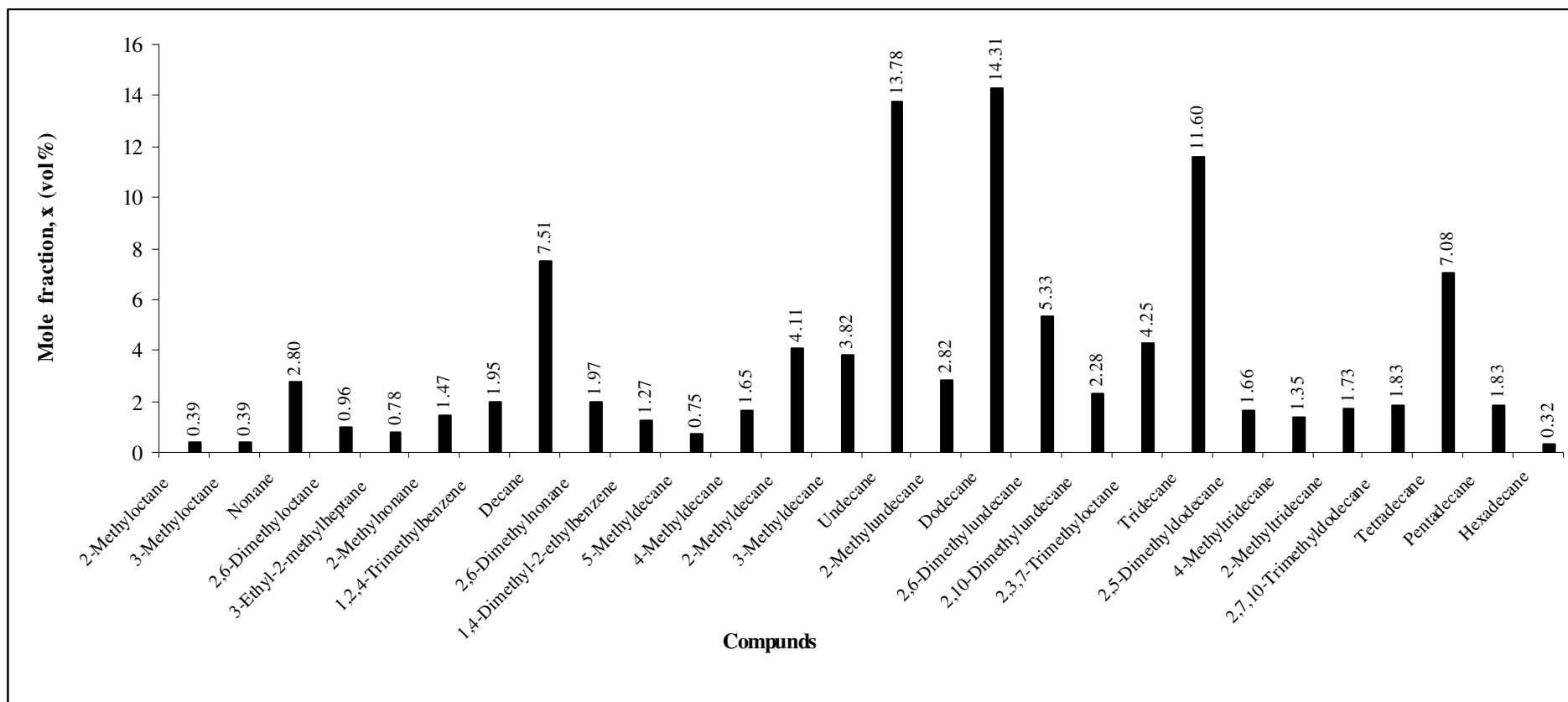


Fig. 3. Mole fractions of the selected 28 hydrocarbon components in the liquid phase.

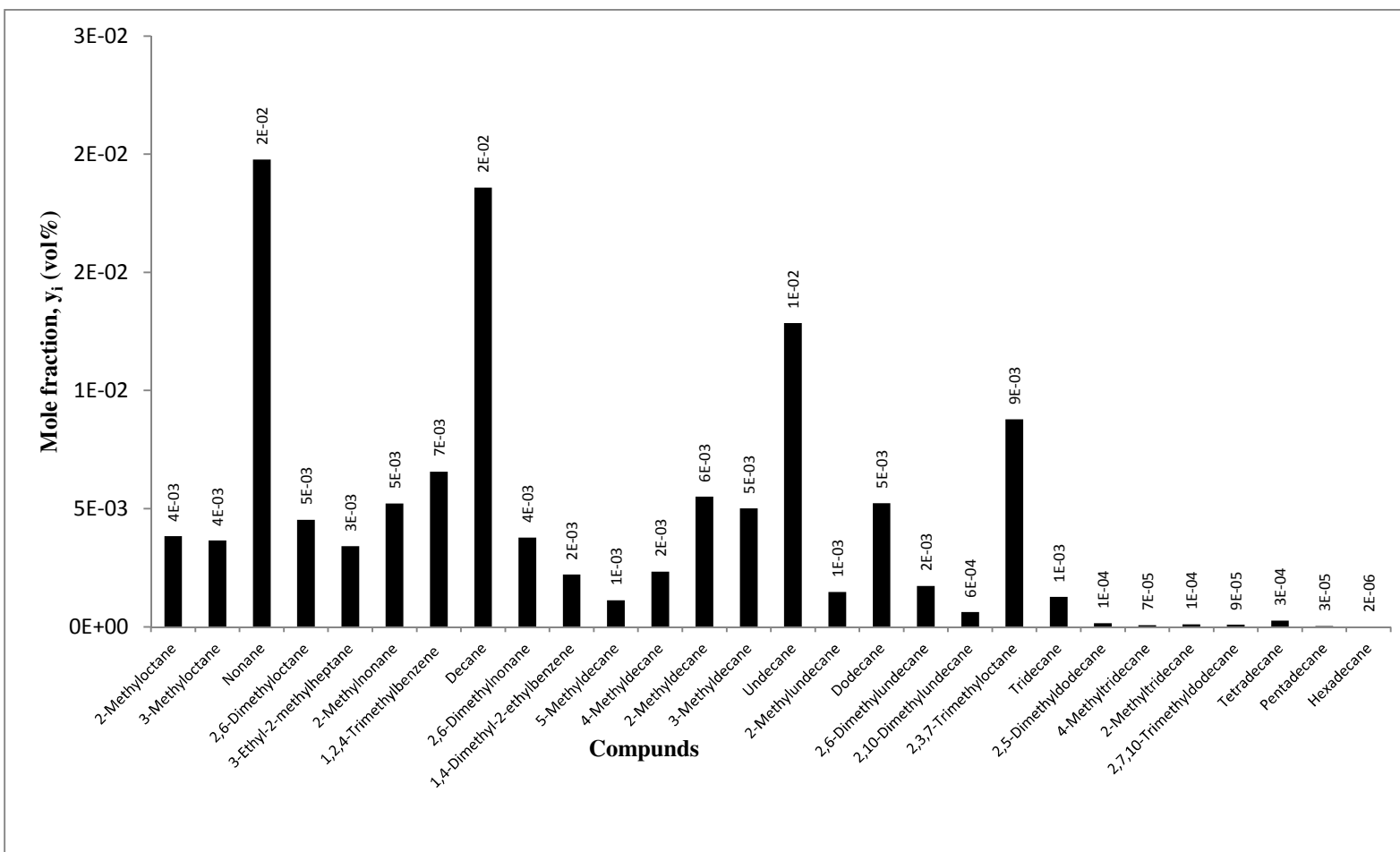


Fig. 4. Mole fractions of the selected 28 hydrocarbon components in the vapour phase.

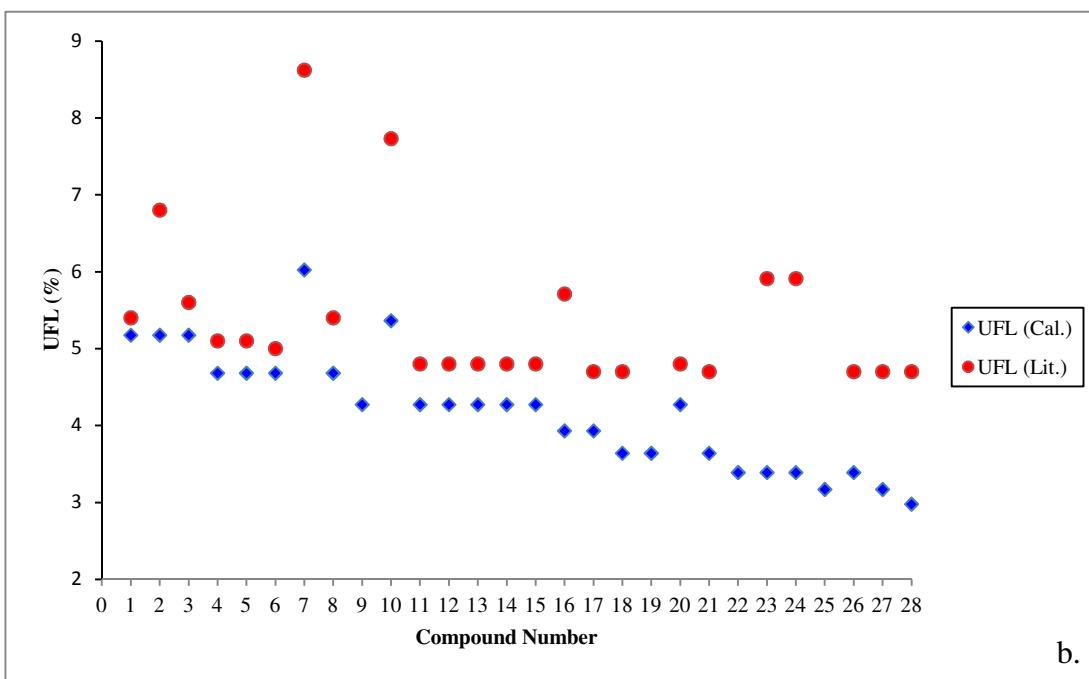
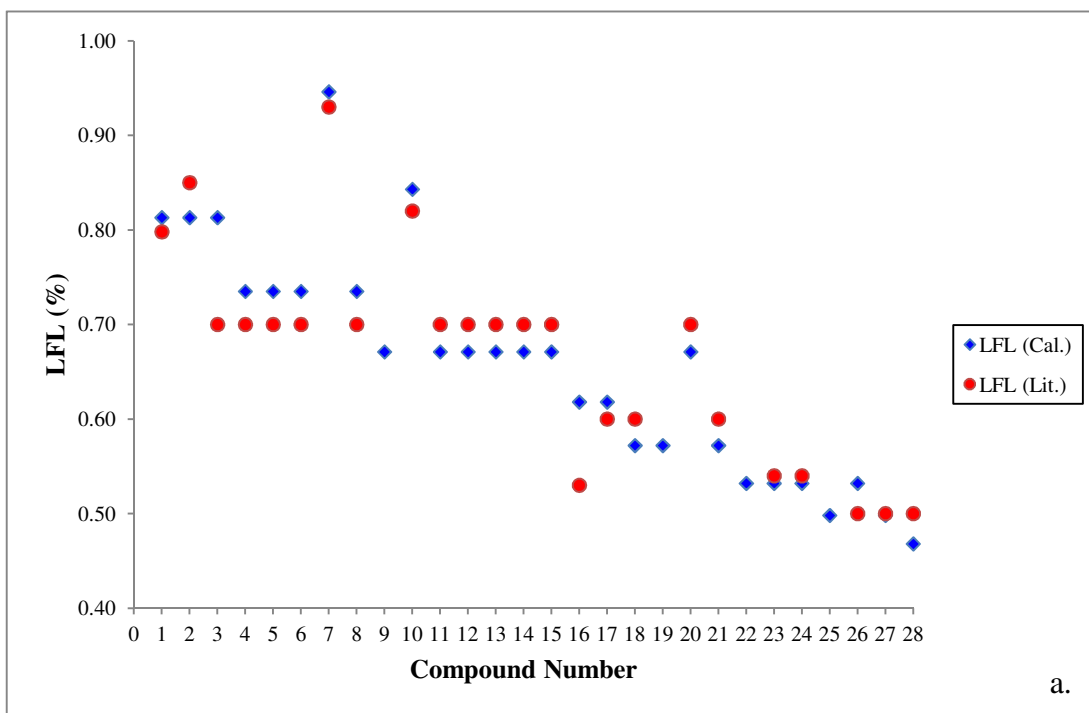


Fig. 5a &b. Comparison between calculated and literature values of *LFL* and *UFL*.

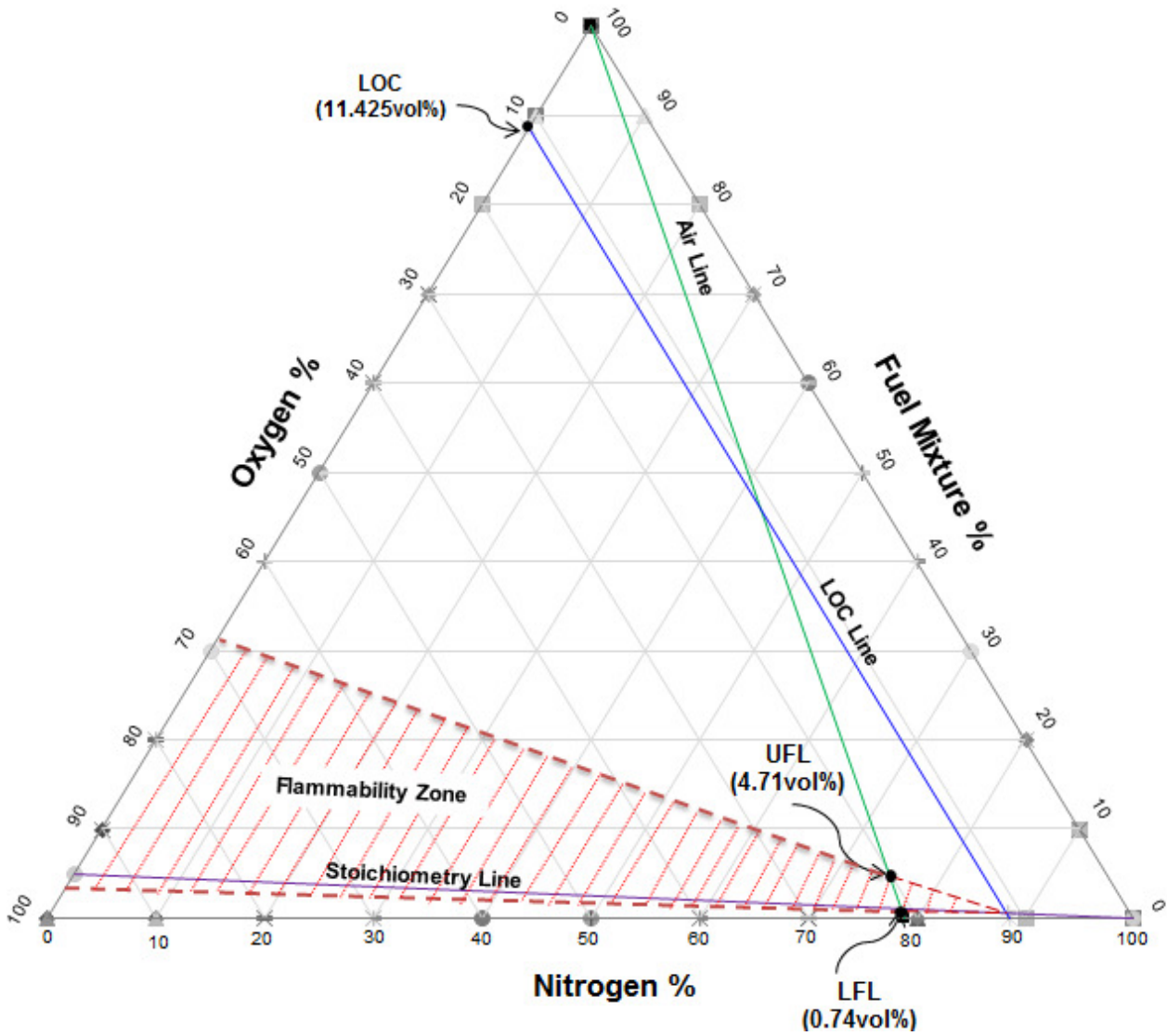


Fig. 6. Triangular flammability diagram of the hydrocarbon mixture.